



A Study of Alginate-Chitosan-Nanoparticles Loaded with Resveratrol for Inhibition of Melanoma Cells

Pei-Ru Chen

Department of Biomedical Engineering, Ming Chuan University, Taiwan, R.O.C

Abstract Cancer is one of the diseases that everyone can get, because the destruction of the ozone layer makes the ultraviolet rays irradiated on the surface soaring, and the skin cells exposed to ultraviolet rays have a certain probability that the DNA will be damaged and the disease will become skin cancer. Resveratrol was found in the literature and confirmed that this phenolic substance has a positive effect on breast cancer, skin cancer, gastric cancer, rectal cancer, esophageal cancer, prostate cancer, pancreatic cancer and leukemia. Therefore, this research mainly discusses the nanoparticles prepared by ionotropic pre-gelation and polycation cross-linking with using natural polymers-alginate and chitosan and load different concentrations of resveratrol solution into nanoparticles. The nanoparticles produced at present have an average particle size between 420 and 490 nm, and the distribution rate is controlled at 0.2 to 0.45 (Mw / Mn). The MTT test has a slight effect on NIH 3T3 fibroblasts at first. Afterwards, they all grow normally and have inhibitory effect on B16F10 melanoma cells. In the cell migration experiment, the inhibitory effect of resveratrol-loaded nanoparticles was obvious at the 24th hour, and at the 48th hour, the control group and the unloaded nanoparticle group were compared with the drug-loaded nanoparticle groups' B16F10 melanoma cells grew faster so it was inferred that the drug-loaded nanoparticles could inhibit the growth of B16F10 melanoma cells.

Keywords Resveratrol, Alginate, Chitosan, Nanoparticles.

Introduction/ Background

Melanoma is a type of skin cancer originating from melanocytes, characterized by its aggressive behavior and propensity for metastasis [8], poses a significant public health challenge worldwide due to its increasing incidence and high mortality rates [1]. Current treatment options for melanoma, including surgery, chemotherapy, and immunotherapy, face challenges such as drug resistance, toxicity, and limited efficacy against metastatic disease [9]. Despite advancements in therapeutic approaches, the management of metastatic melanoma remains challenging, necessitating the exploration of therapeutic approaches that are both effective and safe [2].

Nanotechnology has emerged as a promising field for cancer therapy, offering precise targeting of therapeutic agents to tumor cells while minimizing systemic toxicity [3]. Nanoparticle-based drug delivery systems offer advantages such as targeted delivery, improved bioavailability, and reduced systemic toxicity [11]. Alginate-chitosan nanoparticles (ACNPs) have garnered attention as drug delivery carriers due to their biocompatibility, biodegradability, and ability to encapsulate a wide range of bioactive compounds and protect them from degradation and enabling controlled release at the target site [4].

Resveratrol, a natural polyphenol found in grapes, berries, and peanuts, has demonstrated potent anticancer properties, including inhibition of cell proliferation, induction of apoptosis, and suppression of metastasis in various cancer types [5]. Resveratrol, a natural polyphenol, has demonstrated anticancer effects, including inhibition of melanoma cell growth, induction of apoptosis, and suppression of angiogenesis and metastasis [10]. Preclinical studies have demonstrated the efficacy of resveratrol against melanoma cells through various mechanisms, including modulation of signaling pathways and induction of apoptosis [14]. However, its clinical application has been limited by poor bioavailability and rapid degradation [6].



Encapsulation of resveratrol within nanoparticles has been shown to enhance its stability, solubility, and bioavailability, leading to improved therapeutic efficacy [13]. Alginate-Chitosan-Nanoparticles (ACNPs) have been explored as carriers for various anticancer agents, offering advantages such as prolonged circulation time and targeted delivery to tumor sites [15]. The combination of resveratrol's anticancer properties with the advantages of ACNPs as drug delivery carriers presents a rational approach for enhancing the efficacy of melanoma treatment [17]. This research aims to investigate the efficacy of Alginate-Chitosan-Nanoparticles (ACNPs) loaded with resveratrol in inhibiting melanoma cells. The encapsulation of resveratrol within ACNPs is hypothesized to enhance its bioavailability and therapeutic efficacy against melanoma, offering a promising approach for melanoma treatment [7].

In this study, we aim to prepare and characterize Alginate-Chitosan-Nanoparticles (ACNPs) loaded with resveratrol and evaluate their efficacy in inhibiting melanoma cell proliferation, inducing apoptosis, and suppressing metastasis both in vitro and in vivo. By elucidating the therapeutic potential of these novel formulations, we hope to contribute to the development of effective and safe strategies for melanoma treatment.

Materials and Methods

A. Preparation of Resveratrol unloaded Alginate-Chitosan-Nanoparticles (ALG-CS)

Three solutions were prepared as followed : (A) Sodium alginate solution: 0.074g sodium alginate + 117.426ml deionized water (pH adjusted to 4.9), (B) Calcium chloride solution: 0.015g calcium chloride + 7.485ml deionized water and (C) Chitosan solution: 0.0125g chitosan + 24.9875ml acetic acid (pH adjusted to 4.6)

Adding solution (B) into solution (A) to obtained calcium alginate pre-gel. Then, slowly adding solution (C) at a constant rate of 40ml/hr (mixing process carried out under magnetic stirring at 600rpm for 45 minutes). After stirring, adjust the pH of mixing solution to 7.2 ~ 7.4, then centrifuged at 13200rpm for 20 minutes at 4°C. Finally, nanoparticle solution was collected from the supernatant.

B. Preparation of Resveratrol loaded Alginate-Chitosan-Nanoparticles (ALG-CS-RES)

By varying the concentration of resveratrol (1.0mg, 3.0mg, and 5.0mg/1ml ethanol), different resveratrol-sodium alginate-chitosan nanoparticles can be prepared. First, dissolve resveratrol in ethanol to prepare solutions with concentrations of 1.0mg/ml, 3.0mg/ml, and 5.0mg/ml, respectively. Then, replace the deionized water in the preparation of calcium chloride solution with the resveratrol solution. Afterward, follow the same process as preparing resveratrol unloaded nanoparticles to obtain three different resveratrol concentrations of resveratrol-sodium alginate-chitosan nanoparticles.

C. Size analysis of Alginate-Chitosan-Nanoparticles

Adding the prepared four types of nanoparticles including resveratrol unloaded and loaded sequentially into quartz tubes and analyze them using a particle size analyzer. Perform three repeated tests to determine the average particle size and polydispersity index (PDI) of the nanoparticles.

D. Encapsulation rate of resveratrol-loaded alginate-chitosan-Nanoparticles

To prepare the resveratrol standard solution (1mg/ml) and dilute it sequentially to 100%, 50%, 25%, 12.5%, 6.25%, and 0%, then measure the absorbance at 306nm using ELISA to create a standard curve. After centrifuging the three different concentrations of resveratrol-loaded nanoparticles (1.0mg, 3.0mg, and 5.0mg) at 13200rpm for 40 minutes, the absorbance of each sample using ELISA reader was measured. Then using the absorbance values and the standard curve to calculate the unencapsulated resveratrol quantity for each sample. Finally, using the following equation to estimate encapsulation rate:

$$\text{Encapsulation Efficiency(\%)} = \frac{\text{Total Resveratrol} - \text{Unencapsulated Resveratrol}}{\text{Total Resveratrol}} \times 100 \% \quad (1)$$

Where total Resveratrol is the initial amount of resveratrol added to prepare nanoparticles. Unencapsulated Resveratrol is the amount of resveratrol found in the supernatant after centrifugation. The encapsulation rate for each sample was calculated using the provided formula.

E. Release rate of resveratrol-loaded alginate-chitosan-nanoparticles

$$\text{Release Rate(\%)} = \frac{\text{absorption value corresponding to the released drug concentration}}{\text{total drug concentration}} \times 100 \%$$



F. Cell studies

The murine melanoma cell line B16F10 cells were used as model cells and used for the following studies. The B16F10 melanoma cells were cultured in DMEM culture medium containing 10% fetal bovine serum, 3.7 mg/ml sodium bicarbonate, 1% penicillin/streptomycin and 13.48g/L Dulbecco's modified Eagle's medium (DMEM) culture medium solution. Then, B16F10 cells were incubated at 37 °C and in a humidified atmosphere containing 5 % CO₂.

The cell viability of B16F10 melanoma cells and NIH 3T3 fibroblast cells cultured with resveratrol-loaded alginate-chitosan-nanoparticles was evaluated by a standard MTT (3-(4, 5-dimethylthiazol-2-yl)-2, 5-diphenyltetrazolium bromide) assay, which is a quantitative colorimetric assay for determining the level of cell growth and proliferation. In the beginning, B16F10 cells were seeded onto a 96-well plate (5000 cells/well). Next, once cell adherence was confirmed, the old culture medium was replaced with a fresh medium containing 0.2ml of drug-loaded nanoparticles (drug-loaded nanoparticles: culture medium = 1:9). Cell activity was recorded on days 1, 3, and 7 post-incubation. To perform the MTT assay, the culture medium was discarded, and 10 μ l MTT stock solution was added into each well and incubated for another 4 h in the dark. Then, 50 μ l DMSO solution was added into each well to dissolve formazan crystals into a colored solution. The absorbance of the colored formazan solution was measured by an ELISA microplate spectrometer at 570 nm.

The cytotoxicity of B16F10 cells and NIH 3T3 fibroblast cells cultured with resveratrol-loaded alginate-chitosan-nanoparticles was assessed by LDH assay, a quantitative colorimetric assay to measure lactate dehydrogenase (LDH), an enzyme released upon cell death and lysis. To perform the LDH assay, the 100 μ l culture medium was transferred to a fresh 96-well plate, and 100 μ l LDH reagent mixing solution was added into each well and incubated for 30 min in the dark. Then, 50 μ l of stop solution was added to each well, and the absorbance of the medium solution was measured by ELISA microplate spectrometer at 490 nm within 1 hour after adding the stop solution.

The Alizarin red assay was used to determine, quantitatively by colorimetry, the degree of cell calcification. The intracellular or extracellular calcific deposition both indicated the death of cells. The procedure of the Alizarin red assay was as follows. The 10000 B16F10 cells and NIH 3T3 fibroblast cells were seeded in 24 well plates and cultivated with resveratrol-loaded alginate-chitosan-nanoparticles with different resveratrol concentration of was added into each well for 24 h, 48 h, and 72 h incubation. After incubation, the culture medium was discarded, and the cells were washed gently three times with PBS solution. After fixing the cells with 4% formaldehyde for 15 min at room temperature and washing the cells two times with PBS solution, 1 ml of 40 mM ARS was added into each well, and the cells were incubated for 30 min at room temperature. When the incubation was finished, the cells were washed three times with PBS buffer solution to remove ARS dye and then imaged with a microscope.

The cell migration assays were performed by seeding 10000 B16F10 cells in 24 well plates and cultivated with 1 ml DMEM contains 10% FBS in 37 °C incubator for 24 h. Then artificial wound is scratched into the cell monolayers with a sterile plastic 1000 μ l micropipette tip resulting in a 900 μ m gap in the monolayer. Then, resveratrol-loaded alginate-chitosan-nanoparticles with different resveratrol concentration was added into each well for 24 h, 48 h, and 72 h incubation. The migration of cells and closure of the gap were observed and recorded by microscope after cell incubation with plasma-treated culture medium. The recorded images were used for the analysis of the cell gap closure ratio by free imaging processing software, Image J.

Results & Discussion

The resveratrol-loaded alginate-chitosan-nanoparticles' size and distribution were determined by a particle size analyzer and the results of nanoparticles size and distribution were shown in Figure 1. The results of four different concentrations of resveratrol (0mg, 1.0mg, 3.0mg, and 5.0mg/ml) after three repetitions showed that the particle size (Z-Average) of the resveratrol-unloaded nanoparticles was 428.6 nm, while the resveratrol-loaded nanoparticles had a particle size of approximately 460-490 nm. This indicates that encapsulating resveratrol in nanoparticles using this preparation method slightly affects the particle size. The polydispersity index (PDI) represents the molecular weight distribution of nanoparticles. A larger PDI indicates a more uneven distribution, while a smaller PDI indicates a more uniform distribution. In our case, the PDI was controlled to be approximately 0.2 to 0.45 (M_w / M_n), with the PDI range typically being from 0 to 1, and that meant the distribution is neither extremely polydisperse, or broad, nor in any sense narrow.

The dispersive diameter distribution of alginate-chitosan-nanoparticles affects both their degradation time and the release rate of resveratrol loaded within them, with these factors varying according to the nanoparticle diameter. The release rate of caffeine from resveratrol-loaded alginate-chitosan nanoparticles is depicted in Figure 2. The results indicated that the release curve of resveratrol from resveratrol -loaded alginate-chitosan nanoparticles can be



segmented into four distinct stages. The first stage, 0 to 1 h, the average release rate for three different concentration, 36.9 % / h is relatively higher than the other stages. In the second stage, 1 to 3 h, the release rate is very low compared with other stages, and in the third stage, 3 to 24 h, the release rate is 2.23 % / h, in the final stage, 24 to 120 h, the release rate decreases to 0.11 % / h. The rapid release rate observed in the initial stage is due to the accelerated degradation of gelatin nanoparticles with smaller diameters. These smaller nanoparticles possess a higher surface-to-volume ratio, leading to a faster degradation rate. This varied size distribution of caffeine-loaded gelatin nanoparticles can extend the release duration to over 120 hours.

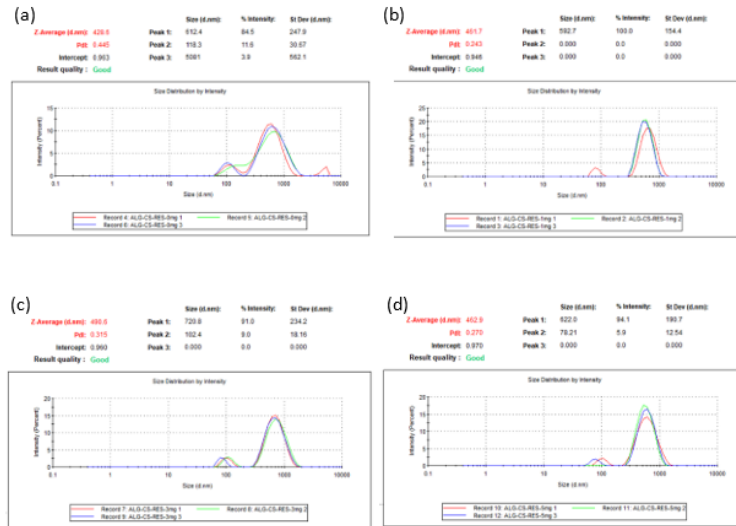


Figure 1: Particles size distribution of (a) resveratrol-unloaded and (b) 1mg/ml, (c) 3mg/ml, (d) 5mg/ml resveratrol-loaded alginate-chitosan-nanoparticles

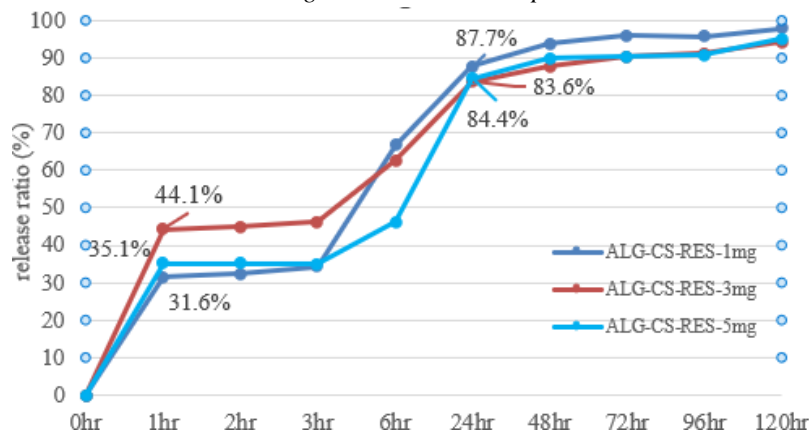


Figure 2: The release rate of caffeine from resveratrol-loaded alginate-chitosan nanoparticles.

The prepared standard resveratrol solution (1 mg/ml) was diluted sequentially to 100%, 50%, 25%, 12.5%, 6.25%, and 0%. Then, the absorbance was measured at wavelength of 306 nm for each dilution to create the standard characterization curve shown in Figure 3. By inserting the absorbance values of the nanoparticle samples (with concentrations of 1, 3, and 5 mg/ml) into the eq. (1), the encapsulation rate of resveratrol in alginate-chitosan-nanoparticles was determined. After substituting the values into the eq (1), the encapsulation efficiency of resveratrol in nanoparticles at each concentration was approximately 20%, 6%, and 4%, respectively. After performing triplicate experiments and calculations, it was found that the nanoparticles prepared by this method could only encapsulate a resveratrol solution at a concentration of 0.2 mg/ml. We hope to encapsulate more resveratrol into the nanoparticles using this method in the future to enhance the drug's utilization.

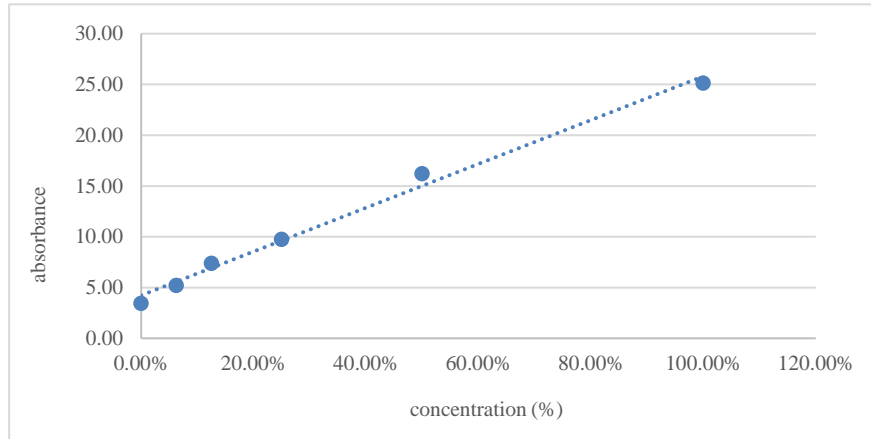


Figure 3: The absorbance of prepared standard resveratrol solution (1 mg/ml) was diluted sequentially to 100%, 50%, 25%, 12.5%, 6.25%, and 0%. The absorbance was measured at wavelength of 306 nm for each dilution to create the standard characterization curve.

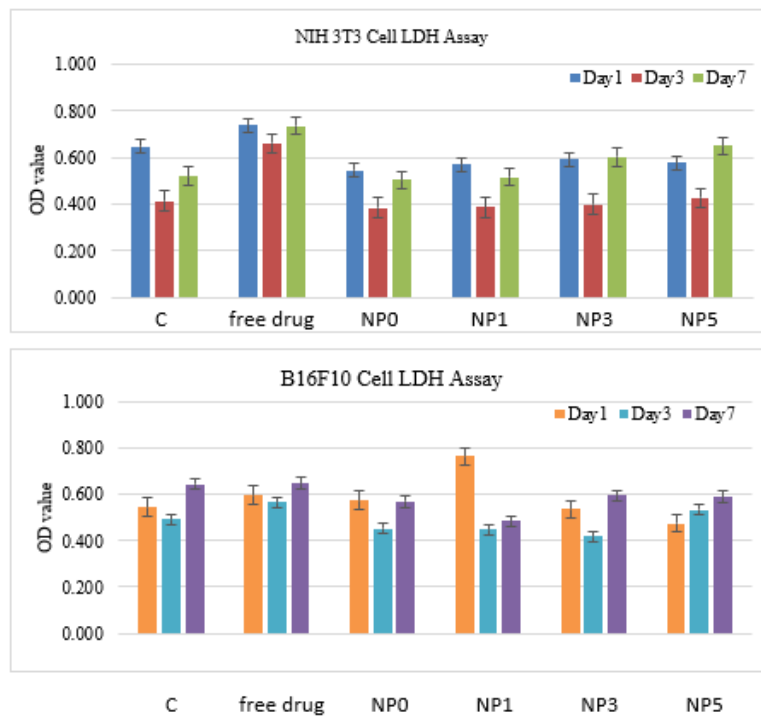


Figure 4: The results of the cell viability of NIH3T3 fibroblasts and B16F10 melanoma cells after the administration of six different drugs

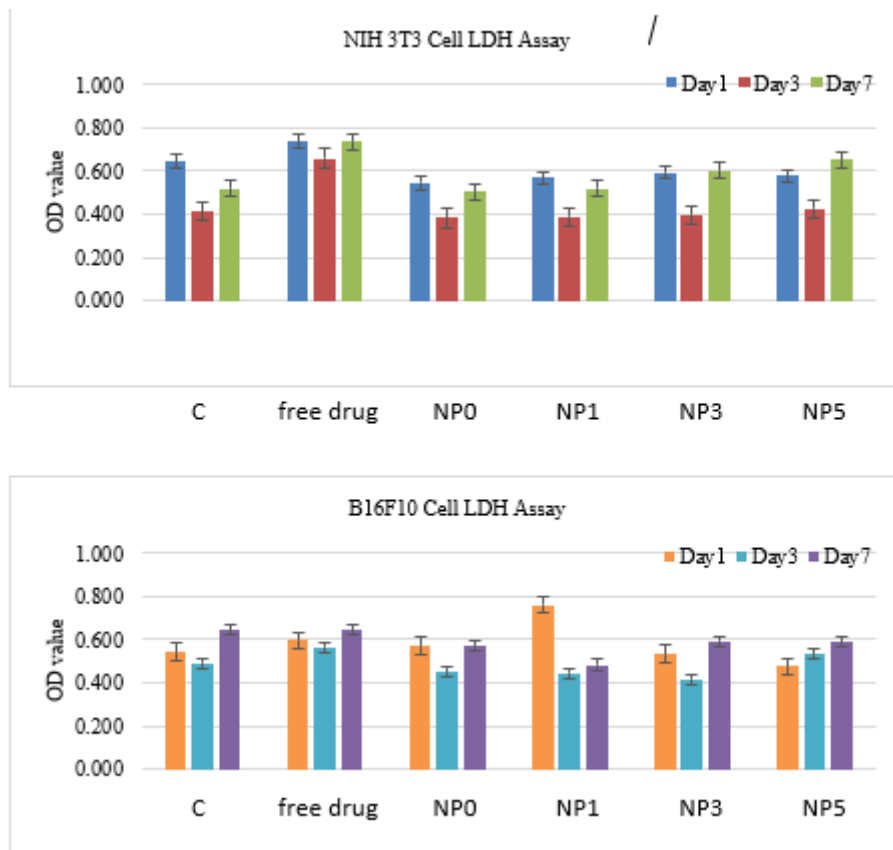


Figure 5: The results of the cell cytotoxicity of NIH3T3 fibroblasts and B16F10 melanoma cells after the administration of six different drugs.

As shown in Figure 4, the results of the cell viability of NIH3T3 fibroblasts and B16F10 melanoma cells after the administration of six different drugs are illustrated. The group “C” is group of control that contains no resveratrol and nanoparticles. The group “free drug” is a group that resveratrol solution (0.2mg/ml) is directly added into the culture medium. And the group “NP0” means that the cells were cultured with resveratrol unloaded alginate-chitosan-nanoparticles. In Figure 4(a), it is observed that the cellular activity results of NP0 are the same as those of the control group. Similarly, NP1, NP3, and NP5, when compared to the control group, also show no inhibitory effects on activity. This figure indicates that both the nanoparticles themselves and the nanoparticles encapsulating resveratrol do not have inhibitory effects on the NIH3T3 fibroblast cells. Additionally, the impact of free resveratrol on NIH3T3 fibroblast cells has also been improved. In Figure 4(b), the results show that the cellular activity of NP0 is the same as that of the control group. However, NP1, NP3, and NP5, when compared to the control group, exhibit a significant inhibitory effect on cellular activity, with the effect becoming more pronounced on the seventh day. These results indicate that the nanoparticles themselves do not have an inhibitory effect on B16F10 melanoma cells, but the resveratrol encapsulated by the nanoparticles reduces the cellular activity of B16F10 melanoma cells.

The results of the cell cytotoxicity of NIH3T3 fibroblasts and B16F10 melanoma cells after the administration of six different drugs are shown in Figure 5. Based on the test results shown in Figures 5, when NIH 3T3 fibroblast cells and B16F10 melanoma cells are cultured together with nanoparticles, the growth of cells with different concentrations of nanoparticles shows no difference compared to the control group. Therefore, it can be inferred that the nanoparticles prepared using this method do not exhibit toxicity to NIH 3T3 fibroblast cells and B16F10 melanoma cells.

Alizarin red is used to stain and identify calcium deposits in cell cultures or tissues. When calcium is present, Alizarin Red binds to these deposits, producing a red-colored pigment. The appearance of calcium deposits, either inside or outside cells, indicates that the cells are undergoing apoptosis, a process of programmed cell death. From the staining results shown in Figures 6(a) and 6(b), it can be seen that when cells undergo apoptosis, a mechanism is triggered that causes calcium ions to be released from the endoplasmic reticulum, leading to an increase in



intracellular calcium ion concentration. This results in the precipitation of calcium ions as calcium phosphate. Alizarin red staining can be used to visualize calcium deposits within the cells. Therefore, from the figures, it is evident that the fibroblasts and melanoma cells treated with nanoparticles show no significant increase in calcium deposits in the fibroblasts after Alizarin red staining, indicating no occurrence of apoptosis. This confirms that cell death is caused by chemical factors rather than physical ones. However, the melanoma cells show a significant increase in calcium deposits, confirming that the nanoparticles carrying resveratrol can induce apoptosis in melanoma cells without affecting the growth of fibroblast cells.

The metastasis of cancer cells involves several steps, including migration, invasion, proliferation, and blood vessel formation. To assess the impact of resveratrol released from alginate-chitosan-nanoparticles on the migration behavior of melanoma cells, a migration assay was conducted. The results, shown in Figure 7, indicate that resveratrol negatively affects the migration and gap closure of melanoma cells. After 24 hours of testing, the drug-loaded nanoparticle groups (NP-1, NP-3, NP-5) were significantly more effective at inhibiting the growth of B16F10 melanoma cells compared to the drug-free nanoparticle group (NP-0). The drug-free nanoparticles did not exhibit any inhibitory effect on the growth of the melanoma cells. In Figure 7, the free drug group (RES) likely caused high toxicity, resulting in the cells becoming spherical after just 6 hours. This suggests that the drug-loaded nanoparticles can slowly release resveratrol, reducing its toxicity while effectively inhibiting the growth of melanoma cells.

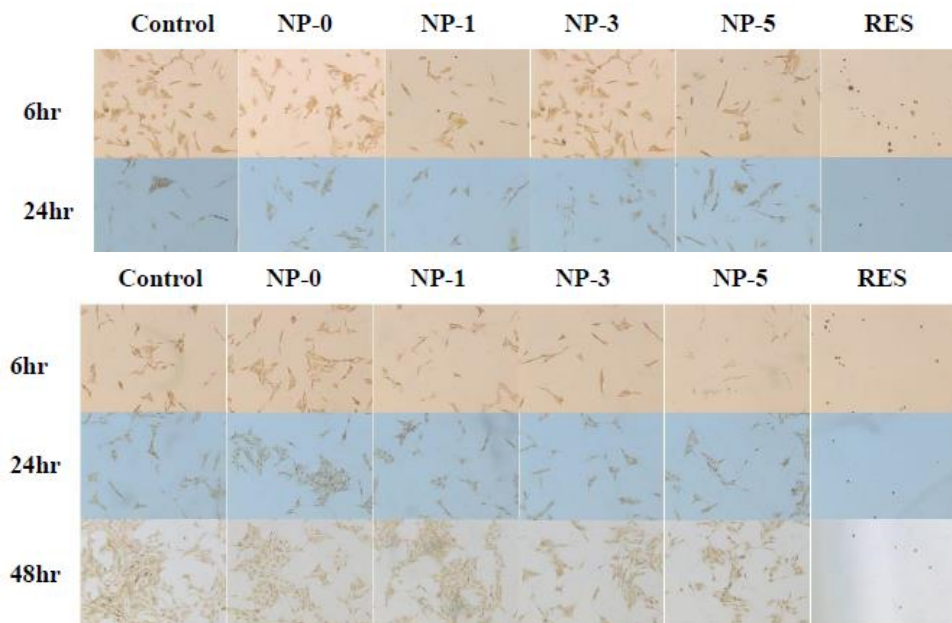


Figure 6: Alizarin red staining results of (a) NIH 3T3 and (b) B16F10 cells under treatment with six different resveratrol unloaded and loaded alginate-chitosan-Nanoparticles for 6, 42 and 72 hrs.

Conclusion

We utilized nanoparticles to encapsulate resveratrol, thereby overcoming various inconveniences associated with its use. We also investigated the inhibitory effects and duration on melanoma cells using the sustained-release properties of nanoparticles. Particle size analysis showed that nanoparticles prepared with resveratrol concentrations of 1, 3, or 5 mg/mL had larger particle sizes compared to drug-free nanoparticles, but the differences among the three concentrations were minimal. The average particle size ranged from 460 to 500 nm, indicating that the resveratrol concentration did not significantly affect particle size.

Regarding encapsulation efficiency, resveratrol concentrations of 1, 3, and 5 mg/mL had encapsulation efficiencies of 20%, 6%, and 4%, respectively, suggesting that the nanoparticles prepared by this method can only encapsulate up to 0.2 mg/mL of resveratrol solution. For release rates, the sustained-release characteristics of the nanoparticles extended the release of resveratrol. The release curve showed two rapid release phases at 0-1 hour and 3-24 hours,



during which most of the resveratrol on the nanoparticle surface and encapsulated within was released, with complete release occurring within 120 hours.

In cell viability experiments, culturing NIH 3T3 fibroblasts with the nanoparticles did not affect cell growth compared to the control group. For B16F10 melanoma cells, the viability of cells in the drug-loaded nanoparticle group was significantly lower than that of the control group as the culture days increased, indicating that these nanoparticles could inhibit the growth of B16F10 melanoma cells without affecting NIH 3T3 fibroblast growth. Regarding cytotoxicity, there were no significant differences between all groups and the control group as the culture days increased, suggesting that the nanoparticles did not exhibit cytotoxicity. The Alizarin Red staining experiment showed calcium deposition in B16F10 melanoma cells treated with drug-loaded nanoparticles, while NIH 3T3 fibroblasts showed no such deposition compared to the control group. Calcium deposition within the cells indicates an increase in intracellular calcium ion concentration, confirming that the cells are undergoing apoptosis. The cell migration experiment results confirmed that drug-loaded nanoparticles could inhibit the growth of melanoma cells. In conclusion, the nanoparticles prepared by this method have stable particle sizes, are biocompatible and non-toxic, and can inhibit the activity of B16F10 melanoma cells. In the future, we aim to increase the encapsulation efficiency and extend the drug release duration to over a week. To effectively apply nanoparticles in vivo, we plan to implement targeted delivery to enhance their effect on specific cells.

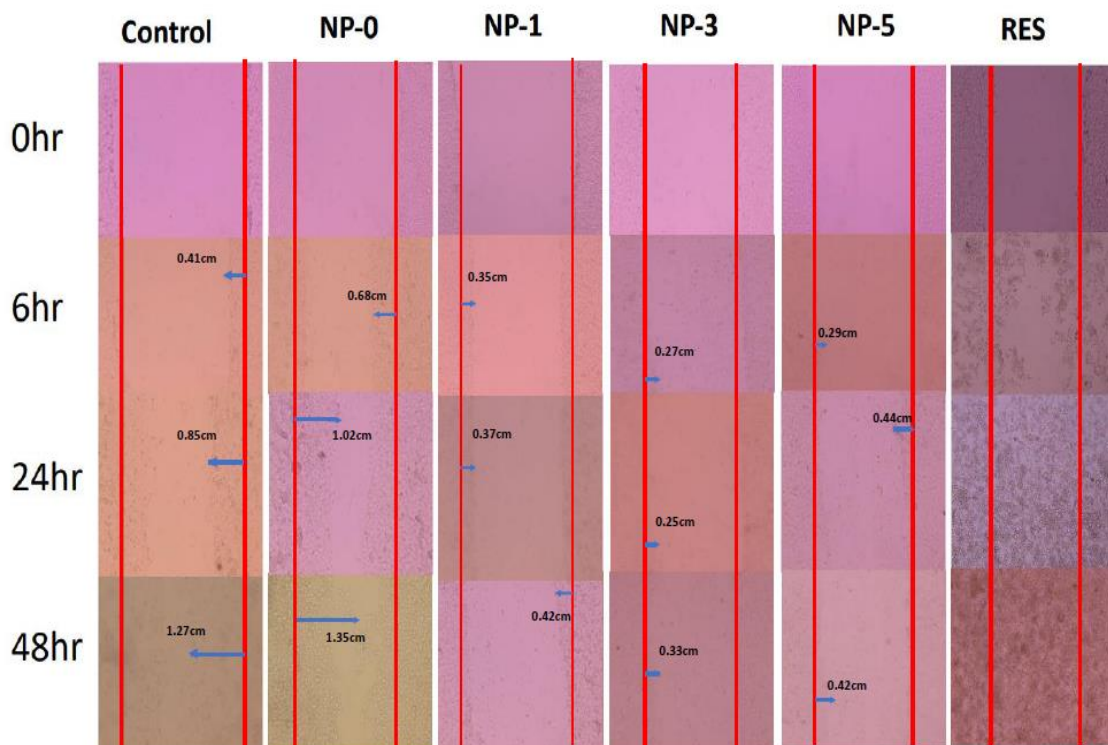


Figure 7: Effects of resveratrol released from alginate-chitosan-nanoparticles on the migration behavior of B16F10 melanoma cells

References

- [1]. Siegel, R.L., et al. (2021). Cancer statistics, 2021. CA: A Cancer Journal for Clinicians, 71(1), 7-33.
- [2]. Long, G.V., et al. (2020). Adjuvant dabrafenib plus trametinib in stage III BRAF-mutated melanoma. New England Journal of Medicine, 383(12), 1130-1140.
- [3]. Farokhzad, O.C., & Langer, R. (2009). Impact of nanotechnology on drug delivery. ACS Nano, 3(1), 16-20.
- [4]. Saeedi, M., et al. (2020). Alginate/chitosan nanoparticles for drug delivery. Journal of Drug Delivery Science and Technology, 56, 101513.
- [5]. Rauf, A., et al. (2018). Health potential of resveratrol: Key mechanisms of action. Nutrients, 10(7), 944.
- [6]. Salehi, B., et al. (2018). Resveratrol: A double-edged sword in health benefits. Biomedicines, 6(3), 91.
- [7]. Kumari, A., et al. (2010). Alginate-chitosan nanoparticles for drug delivery and targeting. International Journal of Pharmaceutical Sciences Review and Research, 5(1), 45-53.
- [8]. Gray-Schopfer, V., et al. (2007). Melanoma biology and new targeted therapy. Nature, 445(7130), 851-857.
- [9]. Singh, C.K., et al. (2015). Resveratrol induces cell cycle arrest and apoptosis with docetaxel in prostate cancer cells via a p53/p21WAF1/CIP1 and p27KIP1 pathway. Oncotarget, 6(14), 1-16.



- [10]. Hosseini, S.F., et al. (2018). Alginate-based nanocarriers for drug delivery applications. *International Journal of Biological Macromolecules*, 120, 472-483.
- [11]. Ríos, J.L., et al. (2018). Melanoma: A relevant model for testing anticancer drugs. *Methods in Molecular Biology*, 1805, 43-52.
- [12]. Farokhzad, O.C., & Langer, R. (2009). Impact of nanotechnology on drug delivery. *ACS Nano*, 3(1), 16-20.
- [13]. Singh, C.K., et al. (2015). Resveratrol induces cell cycle arrest and apoptosis with docetaxel in prostate cancer cells via a p53/p21WAF1/CIP1 and p27KIP1 pathway. *Oncotarget*, 6(14), 1-16.
- [14]. Hosseini, S.F., et al. (2018). Alginate-based nanocarriers for drug delivery applications. *International Journal of Biological Macromolecules*, 120, 472-483.
- [15]. Salehi, B., et al. (2018). Resveratrol: A double-edged sword in health benefits. *Biomedicines*, 6(3), 91.
- [16]. Gray-Schopfer, V., et al. (2007). Melanoma biology and new targeted therapy. *Nature*, 445(7130), 851-857.
- [17]. Ríos, J.L., et al. (2018). Melanoma: A relevant model for testing anticancer drugs. *Methods in Molecular Biology*, 1805, 43-52.
- [18]. Moonesun, M., Javadi, M., Charmdooz, P., & Mikhailovich, K. U. (2013). Evaluation of submarine model test in towing tank and comparison with CFD and experimental formulas for fully submerged resistance. *Indian Journal of Geo-Marine Sciences*, 42(8), 1049-1056.

